ISBN: 978-3-95450-220-2 ISSN: 2673-5474 doi: 10.18429/JACoW-FEL2022-WEP13

DEMONSTRATION OF HARD X-RAY MULTIPLEXING USING MICROBUNCH ROTATION THROUGH AN ACHROMATIC BEND *

R. A. Margraf[†1], J. P. MacArthur, G. Marcus, H.-D. Nuhn, A. Lutman, A. Halavanau, Z. Huang[1]
SLAC National Accelerator Laboratory, Menlo Park, USA
[1]also at Stanford University, Stanford, USA

Abstract

Electrons in a X-ray free electron laser (XFEL) develop periodic density fluctuations, known as microbunches, which enable the exponential gain of X-ray power in an XFEL. When an electron beam microbunched at a hard X-ray wavelength is kicked, microbunches are often washed out due to the dispersion and R_{56} of the bend. An achromatic (dispersion-free) bend with small R_{56}, however, can preserve microbunches, which rotate to follow the new trajectory of the electron bunch. Rotated microbunches can subsequently be lased in a repointed undulator to produce a new beam of off-axis X-rays. In this work, we demonstrate hard X-ray multiplexing in the Linac Coherent Light Source (LCLS) Hard X-ray Undulator Line (HXU) using microbunch rotation through a 10 µrad first-order-achromatic bend created by transversely offsetting quadrupole magnets in the FODO lattice. Quadrupole offsets are determined analytically from beam-matrix theory. We also discuss the application of microbunch rotation to out-coupling a cavity-based XFEL (CBXFEL) [1].

INTRODUCTION

Microbunch rotation using achromatic bends has long been known as an option for for out-coupling infrared FEL oscillators [2], and MacArthur et al. demonstrated a 5 µrad rotation with a single offset quadrupole for soft x-ray microbunches [3]. However, microbunch rotation with hard X-rays has proved more challenging. Shorter microbunches, separated at the radiation wavelength, λ_r, are more sensitive to bunching factor ($\theta \approx (\frac{2\pi}{\lambda_r} + \frac{2\pi}{\lambda_u})z$) degradation due to changes in the z position of the particles relative to the center of the microbunch.

Cavity-based XFELs, such as the X-ray Regenerative Amplifier FEL (XRAFEL) [4, 5] and X-ray FEL Oscillator (XFELO) [6] typically operate Bragg-reflecting cavities at hard X-ray wavelengths. To extend microbunch rotation as an out-coupling mechanism for these cavities, we need to extend it to hard X-rays, such as the 9.832 keV X-ray energy used by the CBXFEL project [1].

MICROBUNCH ROTATION FROM AN OFFSET QUADRUPOLE TRIPLET

MacArthur et al. [3] proposed a triplet of three offset quadrupoles to perform microbunch rotation at hard X-ray wavelengths. Such a scheme is illustrated in Fig. 1, where α is the microbunch rotation angle, f_1, f_2, and f_3 are the quadrupole focal lengths, and L_1, and L_2, are the distances between the quadrupoles.

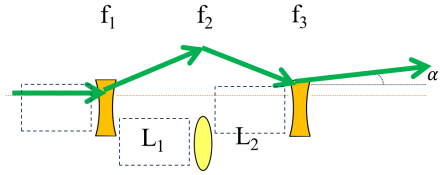

Figure 1: Offset quadrupole triplet for microbunch rotation.

Later work [7, 8] identified microbunch rotation through this triplet is optimized when the kicks from the three quadrupoles form a first-order achromatic bend. To preserve microbunching through a bend, one has to prevent the energy spread of the electron beam from coupling to the longitudinal and transverse dimensions of the beam. In transfer matrix formalism, for a kick in x, these are the R_{16} (Dispersion), R_{26} (Dispersion') and R_{56} elements. An achromatic bend sets the Dispersion and Dispersion' elements to zero. The quadrupole offsets which achieve this can be analytically found. In the thin quadrupole limit, these are [7, 8]:

$$\begin{aligned} o_1 &= \frac{\alpha f_1 f_2}{L_1} \\ o_2 &= \frac{-\alpha f_2 (f_2 L_1 + f_2 L_2 - 2 L_1 L_2)}{L_1 L_2} \\ o_3 &= \frac{\alpha (L_2^2 + f_2 f_3)}{L_2}. \end{aligned} \tag{1}$$

If we implement microbunch rotation in a FODO lattice where $f_1 = f_3 = -f_2$, and $L_1 = L_2 = L$, these simplify to:

$$\begin{aligned} o_1 &= \frac{-\alpha f_1^2}{L} \\ o_2 &= -2\alpha f_1 \left(1 + \frac{f_1}{L}\right) \\ o_3 &= \frac{-\alpha (f_1^2 - L^2)}{L}. \end{aligned} \tag{2}$$

A more lengthy analytical solution also exists in the thick quadrupole limit [7], and this was used to determine the quadrupole offsets for this experiment, which differed by a few µrad from the thin quadrupole values.

To preserve microbunching, we must also keep R_{56} small. An expression for R_{56} through the offset quadrupole triplet

* This work was supported by the Department of Energy, Laboratory Directed Research and Development program at SLAC National Accelerator Laboratory, under contract DE-AC02-76SF00515.
† rmargraf@stanford.edu

ISBN: 978-3-95450-220-2 ISSN: 2673-5474 doi: 10.18429/JACoW-FEL2022-WEP13

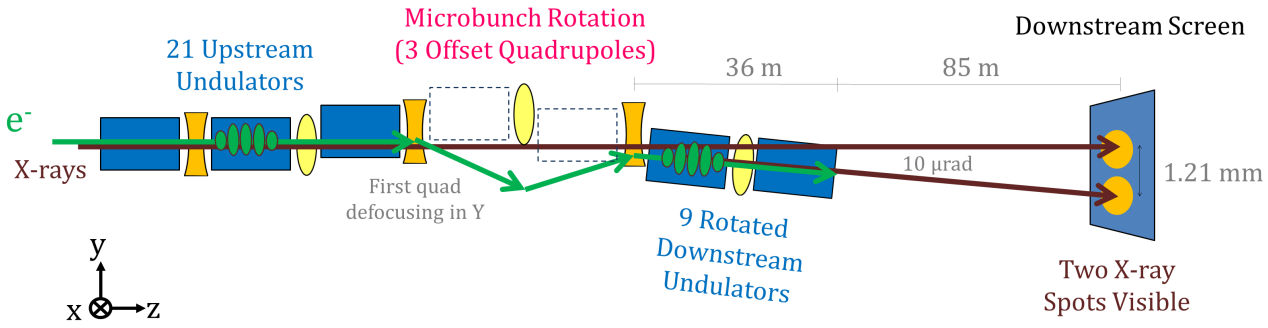

Figure 2: Side view of experimental set-up in LCLS-II Hard X-ray Undulator Hall.

in a FODO lattice is given in Eq. (3) [8]. A smaller R_{56} can be achieved by picking the first quadrupole in the triplet to be defocusing in the dimension of the kick (eg. $f_1 < 1$).

$$R_{56} = \alpha^2 f_1 \left(1 + \frac{2f_1}{L}\right) + \frac{2L}{\gamma^2} \tag{3}$$

To lase the rotated microbunches, one must then align undulators to the new repointed trajectory. One important detail to note is that the electron beam does not fully return on-axis in the third quadrupole. Propagating an on-axis beam through the beam matrices defined in [7] in the thin quadrupole limit for a FODO lattice, one can show the trajectory in the third quadrupole is equal to αL_1. Our entire repointed undulator line is thus offset by this amount.

EXPERIMENTAL DEMONSTRATION

Set-up

A schematic of the experimental set-up, performed using the LCLS-II Hard X-ray Undulator line (HXU) with the 120 Hz Cu linac, is given in Fig. 2. We offset three undulator girders and their associated quadrupoles in Y using the analytically calculated offsets. We chose to kick vertically instead of horizontally because the LCLS-II HXU undulators are horizontal gap, and a vertical shift allowed us to continue to lase in the undulator immediately before the quadrupole triplet, even though that undulator was offset vertically with its attached quadrupole. We repointed the undulators downstream of the offset quadrupoles to the new electron beam trajectory. No scanning of the triplet quadrupole offsets was needed. To maximize power in the repointed spot, we used corrector dipoles to flatten the orbit in the repointed section, and scanned the K of the repointed undulators.

Experimental parameters are given in Table 1. B'_1, B'_3, B'_2 are the quadrupole gradients, L_{Quad} is the effective quadrupole length, L_{Und} is the length of the undulator in each segment, and λ_u is the undulator period. E_{e^-} and E_{λ_r} define the energy of the electron and X-ray beams. $\epsilon_{x,norm}$ is a typical LCLS Cu Linac normalized emittance in the undulator hall. Δt_{FWHM}, I_{core} and $\Delta E_{slice,core}$ define the electron beam pulse duration and the average current and average slice emittance within the central FWHM pulse duration. These last three quantities were calculated from measured time-resolved energy distribution of the electron bunch downstream of the undulator line, without undulator lasing. Time dependent horizontal streaking is provided by an X-ray transverse deflecting cavity (XTCAV).

Table 1: Experimental Parameters

f_1=f_3, f_2	(−12.0, 12.0) m	L_1=L_2	4.013 m
B'_1=B'_3, B'_2	(−35.7, 35.7)T/m	L_{Quad}	8.4 cm
λ_u	2.6 cm	L_{Und}	3.4 m
E_{e^-}	10.79 GeV	E_{λ_r}	10.14 keV
$\epsilon_{x,norm}$ [1]	0.4 × 10^{-6} m*rad	I_{core}	4.38 kA
Δt_{FWHM}	32.7 fs	$\Delta E_{slice,core}$	12.3 MeV

Triplet Quadrupole Offsets: 10 μrad					
o_1	366 μm	o_2	489 μm	o_3	323 μm
Triplet Quadrupole Offsets: 20 μrad					
o_1	733 μm	o_2	978 μm	o_3	646 μm

The final table section defines the quadrupole offsets. Microbunch rotation was demonstrated at 10 μrad and 20 μrad.

Example Images

Figure 3 shows example single-shot images on the downstream screen. Screen coordinates have been converted into the angular separation between the two beams to clearly show multiplexing at 10 μrad and 20 μrad. The mean angular separations between the two rotated spots were (9.9 ± 0.1) μrad and (20.1 ± 0.1) μrad respectively. Both spot separations agree with the theoretical value within the precision of the screen calibration. To accommodate large quadrupole offsets within the range of the undulator girder movers, the on-axis beam was repointed between the 10 μrad and 20 μrad datasets. Without additional tuning, this caused lower power in the on-axis spot in the 20 μrad case. This repointing was additionally important to allow the 20 μrad repointed spot to pass through the aperture on the gas detector. Further repointing could have prevented the rotated spot in B) from being clipped by this aperture.

[1] Typical LCLS Value

ISBN: 978-3-95450-220-2 ISSN: 2673-5474 doi: 10.18429/JACoW-FEL2022-WEP13

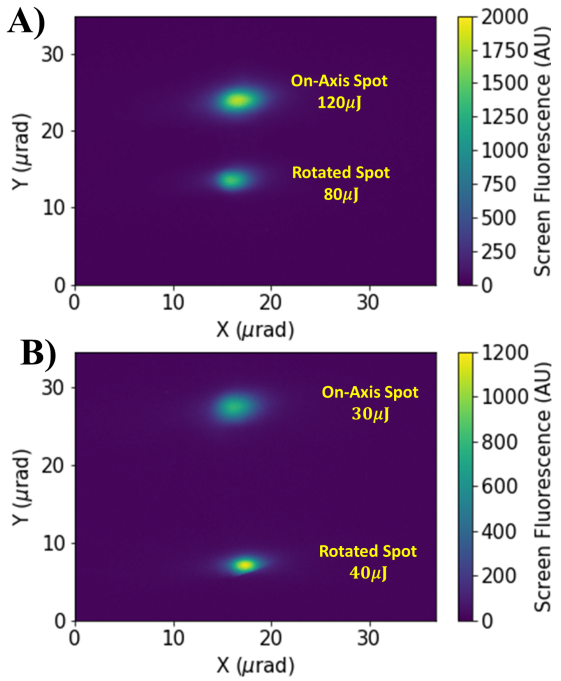

Figure 3: Example single shot microbunch rotation images with average X-ray pulse energies. A) 10 µrad and B) 20 µrad.

K Optimization

We maximized X-ray power by scanning K in the rotated undulator section, as shown in Fig. 4. Our upstream undulators had a linear taper of $\Delta K = -0.0002$ per undulator to compensate for wakefield energy losses in the undulator line. If the average K in the undulator directly upstream of the microbunch rotation triplet was 2.5439, the K following the linear taper for the first repointed undulator would be 2.5435. However, when we scan the repointed undulator section, while keeping the linear taper, we find the optimal K of the first repointed undulator is 2.5396, a detune of -0.15%. Our current simulation efforts, not shown here, suggest the magnitude of this detune is highly dependant on the saturation of the electron beam entering the microbunch rotation triplet. A more highly saturated beam has lost more energy during lasing than a fresh electron beam. We speculate that when the electron beam is separated from the on-axis X-ray beam, the optimal K decreases due to the energy loss from the lasing in the upstream section.

After performing this scan, we added a quadratic taper to the repointed undulator section to further increase power. This quadratic taper is present in the following scans.

Gain in Repointed Undulator Section

We examined the gain in the repointed undulator section by inserting a kick after each repointed undulator, as shown in Fig. 5, with a polynomial fit. We predicted the gain would be quadratic, consistent with superradiant emission [9]. The gain here appears to be primarily linear, with

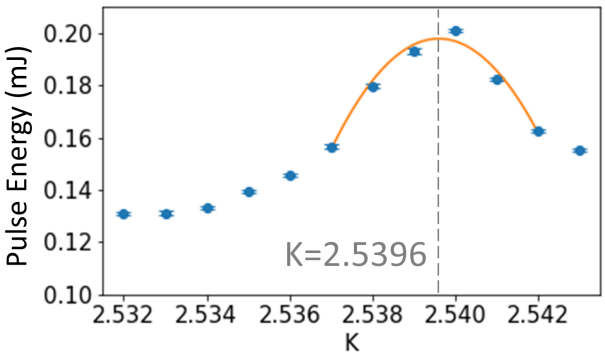

Figure 4: Undulator K scan for the 10 µrad case. The combined pulse energy of the on-axis and rotated X-ray beams was measured on a gas detector as the K of the repointed undulator section was scanned. The gain in the repointed undulator segment varied considerably with K. We optimized K to maximize pulse energy. Error bars give the standard error of the mean.

a quadratic component. Perhaps with further taper optimization, quadratic gain might be possible in future studies.

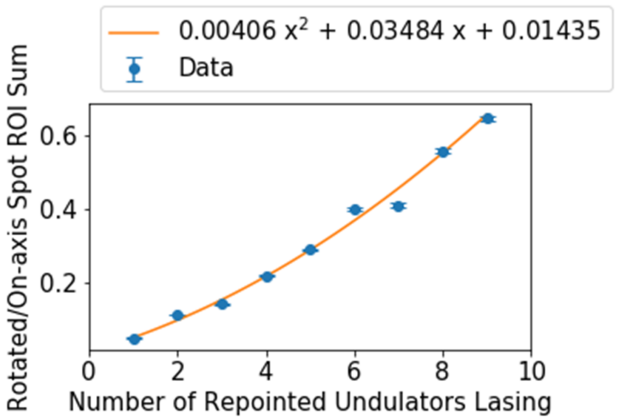

Figure 5: Gain in rotated undulator section for the 10 µrad case. In this run, the power in the on-axis spot was 120 µJ. Error bars give the standard error of the mean.

Phaseshifter Scan

To demonstrate that the gain in the repointed undulator section comes from the microbunching in the electron beam, and not from interaction with the on-axis X-ray seed, we performed a phaseshifter scan, shown in Fig. 6. In a typical on-axis undulator, as in Fig. 6A, using a phaseshifter to delay the electron bunch by 180° relative to the X-ray pulse supresses lasing. However, we find that in the microbunch rotation case, as in Fig. 6B, the power in the repointed undulator section does not change. This suggests there is negligible interaction between the on-axis X-ray beam and the repointed electron beam.

ISBN: 978-3-95450-220-2 ISSN: 2673-5474 doi: 10.18429/JACoW-FEL2022-WEP13

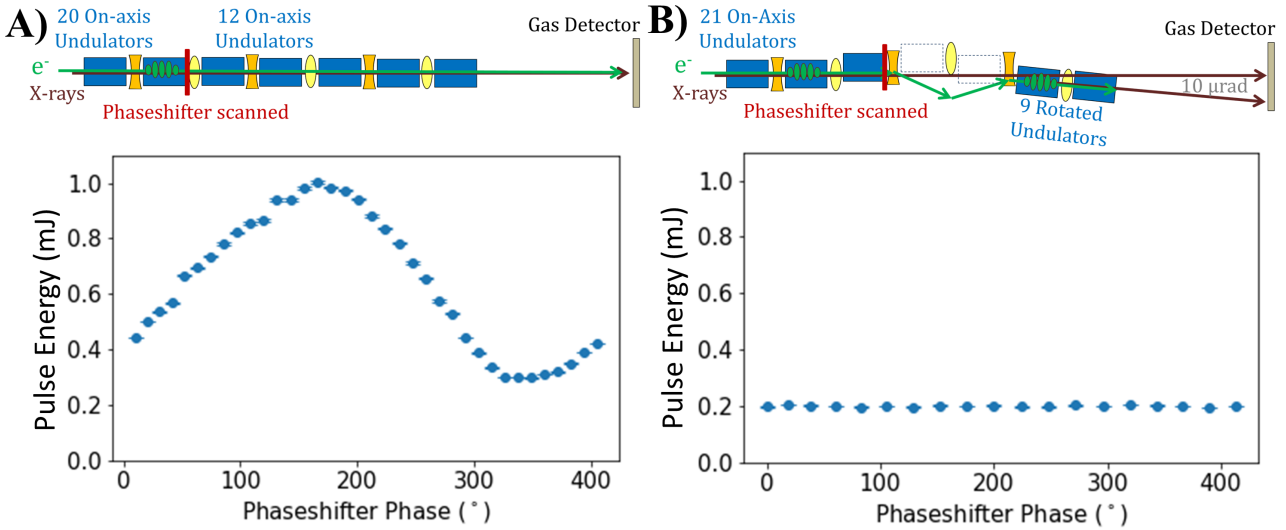

Figure 6: Phaseshifter Scan Demonstration for the 10 µrad case. A) All 32 undulators were aligned on axis, and a phaseshifter was scanned. B) With the microbunch rotation triplet and repointed undulator line installed, the phaseshifter just upstream of the microbunch rotation triplet was scanned. Error bars give the standard error of the mean.

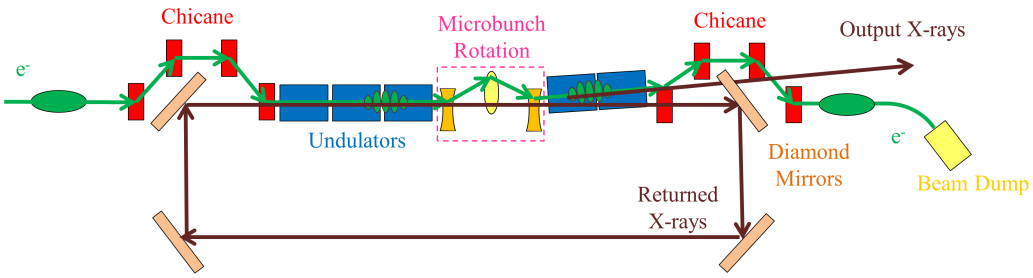

Figure 7: Microbunch rotation as an out-coupling scheme for a cavity-based XFEL.

CONCLUSIONS AND APPLICATIONS TO A CAVITY-BASED XFEL

These results demonstrate microbunch rotation is possible with hard X-ray wavelengths. To our knowledge, this is the first time microbunch rotation has been demonstrated with hard X-rays in the literature. Furthermore, demonstrating microbunch rotation with hard X-ray wavelengths at >10 µrad is significant for the application of microbunch rotation to a cavity-based XFEL.

Proposed cavity-based XFELs [1, 10, 11] use Bragg-reflecting mirrors to circulate X-ray pulses which interact with a series of electron bunches. The CBXFEL project [10] will test a rectangular cavity of diamond (400) Bragg-reflecting mirrors at 9.832 keV, which have an angular reflectivity bandwidth (FWHM) of 8.8 µrad.

A microbunch rotation out-coupling scheme for a cavity-based XFEL is depicted in Fig. 7. X-rays produced by on-axis undulators remain inside the cavity, while re-pointed X-rays miss the rocking curve of the Bragg reflection and are transmitted out of the cavity.

A 10 µrad microbunch rotation is sufficient to miss the Bragg rocking curve of the diamond 400 reflection used by the CBXFEL project. Thus, our demonstration of 10 µrad and 20 µrad rotation of 10.14 keV microbunches supports the feasibility of microbunch rotation for out-coupling a hard X-ray cavity.

In future publications, we will support these experimental results with simulations. Comparing the K detune and gain curve observed here with simulation should provide insight into how to quickly optimize microbunch rotation schemes in the future. We will also continue to consider the applicability of microbunch rotation in upcoming cavity-based FEL projects.

REFERENCES

[1] G. Marcus *et al.*, "Cavity-Based Free-Electron Laser Research and Development: A Joint Argonne National Laboratory and SLAC National Laboratory Collaboration", in *Proc. FEL'19*, Hamburg, Germany, Aug. 2019, pp. 282–287. doi:10.18429/JACoW-FEL2019-TUD04

[2] N.G. Gavrilov, G.N. Kulipanov, V.N. Litvinenko, A.S. Sokolov, and N.A. Vinokurov, "On Mutual Coherency of Spontaneous Radiation from Two Undulators Separated by Achromatic Bend", *IEEE J. Quantum Electron.*, vol. 27, no. 12, pp. 2566–2568, 1991. doi:10.1109/3.104134

[3] J. P. MacArthur, A. A. Lutman, J. Krzywinski, and Z. Huang, "Microbunch Rotation and Coherent Undulator Radiation

ISBN: 978-3-95450-220-2 ISSN: 2673-5474 doi: 10.18429/JACoW-FEL2022-WEP13

from a Kicked Electron Beam," *Phys. Rev. X*, vol. 8, no. 4, p. 041036, 2018. doi:10.1103/PhysRevX.8.041036

[4] Z. Huang and R.D. Ruth, "Fully coherent x-ray pulses from a regenerative-amplifier free-electron laser", *Phys. Rev. Lett.*, vol. 96, pp. 144801, 2006. doi:10.1103/PhysRevLett.96.144801

[5] G. Marcus *et al.*, "Refractive Guide Switching a Regenerative Amplifier Free-Electron Laser for High Peak and Average Power Hard X Rays", *Phys. Rev. Lett.*, vol. 125, no. 25, p. 254801, Dec. 2020. doi:10.1103/PhysRevLett.125.254801

[6] K.-J. Kim, Y. Shvyd'ko, and Sven Reiche, "A proposal for an x-ray free-electron laser oscillator with an energy-recovery linac", *Phys. Rev. Lett.*, vol. 100, p. 244802, 2008. doi:10.1103/PhysRevLett.100.244802

[7] R. A. Margraf, X. J. Deng, Z. Huang, J. P. MacArthur, and G. Marcus, "Microbunch Rotation for Hard X-Ray Beam Multiplexing", in *Proc. FEL'19*, Hamburg, Germany, Aug. 2019, pp. 665–668. doi:10.18429/JACoW-FEL2019-THP036

[8] R. A. Margraf, J. P. MacArthur, G. Marcus, and Z. Huang, "Microbunch Rotation as an Outcoupling Mechanism for Cavity-based X-Ray Free Electron Lasers", in *Proc. IPAC'20*, Caen, France, May 2020, pp. 35. doi:10.18429/JACoW-IPAC2020-WEVIR03

[9] Q. Jia, "Analysis of emissions from prebunched electron beams", *Phys. Rev. Accel. Beams*, vol. 20, no. 7, p. 070702, 2017. doi:10.1103/PhysRevAccelBeams.20.070702

[10] K.-J. Kim *et al.*, "Test of an X-ray Cavity using Double-Bunches from the LCLS Cu-Linac", in *Proc. IPAC'19*, Melbourne, Australia, May 2019, pp. 1887–1890. doi:10.18429/JACoW-IPAC2019-TUPRB096

[11] P. Rauer, "A Proof-Of-Principle Cavity-Based X-Ray Free-Electron-Laser Demonstrator at the European XFEL", Ph.D dissertation, Department of Physics, University of Hamburg, Hamburg, 2022. doi:10.3204/PUBDB-2022-02800